PERMANENT MAGNETS FOR THE CEBAF 24GEV UPGRADE*

S.J. Brooks†, Brookhaven National Laboratory, Upton, NY, USA
S.A. Bogacz, Thomas Jefferson National Accelerator Facility, Newport News, VA, USA

Abstract

An upgrade of the CEBAF facility to double its present energy of 12 GeV has been proposed [1, 2]. To provide double the number of linac passes using the existing five stacked arc beamlines, some beamlines are replaced by fixed-field accelerator (FFA) arcs, allowing multiple energies to pass through the same magnets. A solution is presented in which two of the existing electromagnetic beamlines are replaced with permanent magnet non-scaling FFA arcs, as demonstrated at CBETA [3–5]. The two-stage design reduces peak magnetic field and synchrotron radiation loss compared to using a single stage. FFAs do not pulse their magnets, making permanent magnets a promising and power-efficient technology option. However, the magnetic field requirements are still at the high end of accelerator permanent magnets produced thus far (1.6 T peak on beam), while the magnets must also be combined-function, having a gradient with a dipole offset. Designs using a novel oval aperture and open midplane within an adapted Halbach magnet are presented.

ENERGY RANGES AND STAGES

The 1090 MeV energy gain of the present CEBAF linacs is not increased in this study, although the injector energy is assumed to be upgraded from 123 MeV to 650 MeV. This is because the same set of linac quadrupoles focusses all transmitted beam energies, so the ratio of maximum-to-minimum beam energy in the first linac should not get too large. The easiest way to do this is to raise the injector energy; it may be done by running the present injector at 110 MeV and adding a two-pass conventional loop through three 90 MeV RF modules, giving $110 + 2 \times (3 \times 90) = 650$ MeV. This is a simplification of the option explored previously in [1].

CEBAF at present has five stacked 180° electromagnetic arcs on either side of the oval-shaped facility and this paper explores replacing either one or two of the highest energy lines by FFA arcs. Limited vertical space in the CEBAF tunnel makes it difficult to add a sixth line of any sort, so each multi-pass FFA removes an electromagnetic line. To double the energy, the total arc passes on each side of the machine is increased from 5 to 11, remembering the final linac pass after all the arcs boosts the energy by an additional 'half turn' (∼1 GeV) and the synchrotron radiation loss at higher energy removes about the same. The resulting numbers of arc passes and energy ranges are given in Table 1.

There is significant overlap between the FFA1 and FFA2 energy ranges because CEBAF physics requires a continuously-tunable energy range. In the electromagnetic lines this is accomplished by scaling the magnet currents with the linac energy gain. The FFAs are made of permanent magnets, so must accommodate any energy from any linac setting. Letting the linac energy range from 925–1090 MeV provides enough adjustment that the lowest possible energy of one FFA turn always coincides or overlaps with the highest energy of the previous turn, but this lowers the lowest energy of the FFA2 arc to below the FFA1 maximum.

Table 1: Energy Ranges of Electromagnetic and FFA Lines

Number of FFA Stages	E/M passes	FFA1 passes	FFA2 passes
None (current)	5	—	—
One	4	7	—
Two (4+4)	3	4	4
Two (5+3)	3	5	3
Energy ranges (GeV)			
None (current)	1.2–11	—	—
One	1.5–9.4	8.9–23	—
Two (4+4)	1.5–7.2	7.1–16	14–23
Two (5+3)	1.5–7.2	7.1–18	16–23

ARC CELL CONSTRAINTS

An optimisation was performed to try and find arc cells with minimal maximum field on any energy's closed orbit centroid. The constraints are given in Table 2.

Table 2: Constraints on FFA Arc Cell Optimisation

Parameter	Value	Unit
Cell angle	2	° clockwise
Radius of curvature	80.6	m
⇒ Cell length	2.81347	m
Both drift lengths	0.1	m
⇒ Packing factor	0.929	
Maximum tune	0.425	cycles/cell
Minimum tune	0.025	in either plane

The cell lattice is BF-O-BD-O using combined function magnets in all cases. The allowable cell tune range is generous to allow the full energy range from linac adjustment.

ARC CELL LATTICES

The parameters of the resulting optimised lattices, for all three options (and both FFAs for the options that have two FFAs), are shown in Table 3. The 'reference energy' implies a beam rigidity ($B\rho$) that can be used to derive the central dipole field given each magnet's bend angle and length.

* Work supported by Brookhaven Science Associates, LLC under Contract No. DE-SC0012704 with the U.S. Department of Energy.
† sbrooks@bnl.gov

Table 3: Optimised Arc Cell Lattices for Different Options

Parameter	One FFA	4+4 FFA1	4+4 FFA2	5+3 FFA1	5+3 FFA2	Unit
Reference energy	15.95	11.55	18.5	12.55	19.5	GeV
BF length	1.36109	2.09794	1.68482	1.57127	1.49155	m
BF angle	-0.05722	-1.73802	-1.14623	-0.65227	-0.98835	°
BF gradient	-48.649	-29.73	-65.616	-35.135	-80.781	T/m
BD length	1.25238	0.51553	0.92865	1.0422	1.12192	m
BD angle	-1.94278	-0.26198	-0.85377	-1.34773	-1.01165	°
BD gradient	43.393	93.393	86.787	42.943	76.276	T/m

ARC CELL PERFORMANCE

The lowest maximum fields achieved for each option are shown in Table 4, along with the total synchrotron radiation (SR) loss in all arc passes. The resulting final energies are just $650 + 11 \times 2 \times 1090 = 24630$ MeV minus the SR loss.

Table 4: FFA Cells Performance Comparison

Number of FFA Stages	Max Field (T)	SR Loss (MeV)	Final Energy (MeV)
One	2.007	1211.48	23418.52
Two (4+4)	1.495	964.44	23665.56
Two (5+3)	1.489	935.30	23694.70

The dependence of maximum field on beam energy is shown in Fig. 1. In all FFAs considered, the maximum field for low energy orbits occurs at the ends of the BD magnet and for high energy orbits near the centre of the BF magnet, with a V-shaped minimum where the switch occurs.

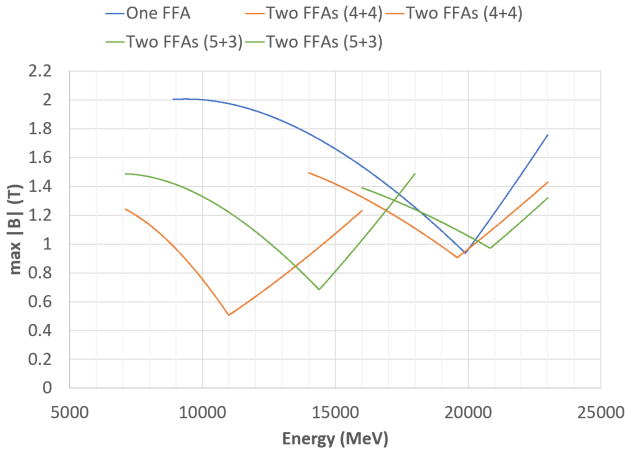

Figure 1: Maximum field on beam centroid, as a function of energy in the various FFA options.

The optimiser tries to balance the maximum field at the high and low ends of the energy range, a task that is made easier by having a smaller energy range, as in the two-FFA options. For the 4+4 turn arrangement, FFA2 has the higher field, which motivated investigation of the 5+3 turn alternative, where the smaller energy range in FFA2 means FFA1 has a slightly higher field.

The SR loss shown in Fig. 2 tells a similar story of the FFAs being better optimised when the energy range is split into two smaller parts. The area under the one-FFA curve is larger and wasteful at low energies. The curve shapes come from the 'γ^4 law' modulated by the orbits being straighter in the middle of the FFA energy range, forming a dip.

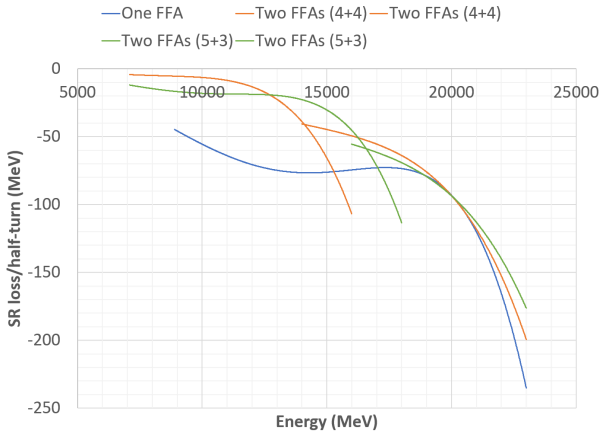

Figure 2: Energy lost to synchrotron radiation in different FFA options.

Finally, a feature of FFA lattices is that different energies go on different orbits, which may have different lengths. This is the case here, as Fig. 3 shows there can be a 3–12 cm path length difference through a given 180° FFA arc.

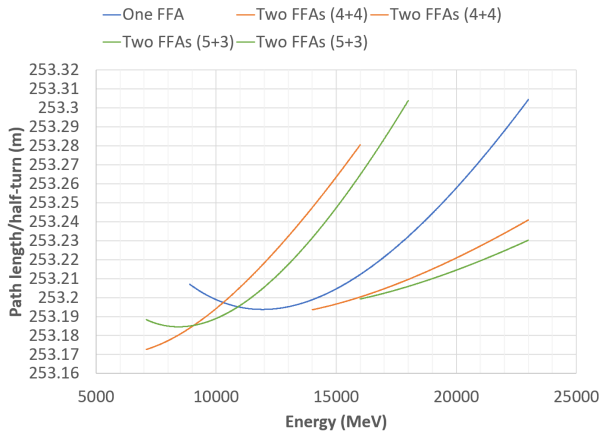

Figure 3: Path length through 180° of arc, as a function of energy in each FFA option.

PERMANENT MAGNETS

Permanent magnets were designed for the two-FFA, 5+3 turn option with the highest performance. The requirements in Table 5 differ in dipole from Table 3 because each magnet's local x has been defined relative to the centre of the orbit excursion in that magnet.

Table 5: Magnet Parameters for the Two-FFA (5+3) Option

Magnet	**Dipole (T) @ $x = 0$**	**Gradient (T/m)**	**x Aperture Range (mm)**
FFA1 BF	-0.52616	-35.135	±27.39
FFA1 BD	-0.73168	42.943	±19.53
FFA2 BF	-0.80051	-40.390	±14.95
FFA2 BD	-1.06879	38.138	±10.66

The gradients for FFA2 have also been halved to make practically-sized apertures possible in all magnets. These small-angle FFA cells can be scaled to half gradients, doubled beam excursions and $\sqrt{2}\times$ cell lengths and angles without affecting the tunes.

The magnet designs include open midplanes to allow synchrotron radiation to escape and use an oval-shaped modified Halbach design for greater efficiency with a horizontal orbit span, following [6]. There are also minimum aperture requirements, all given in Table 6.

Table 6: Permanent Magnet Design Rules

Parameter	**Value**	**Unit**
Material	NdFeB	
Grade	N42EH	
Remnant field B_r	1.30	T
Central aperture gap	20	mm
Midplane slot gap	8	mm
Number of wedges	24 (12 per side)	
Wedge angles (FFA1,2)	30/7.5/30, 20/10/20	°

The cross-sections of the resulting magnet designs are given in Fig. 4. The magnets have cross-sectional areas from 72.8–107.1 cm^2 and harmonic errors from 18.6–30.8 units on any of the small circles shown in the figure. This is within the range correctable by the tuning methods in [5].

Figure 5 shows the areas in the magnet most sensitive to demagnetisation from elevated temperature or radiation. The FFA1 BD magnet was chosen as an example because it has the highest nominal field of 1.571 T in the aperture, although the beam never quite sees this as the orbit exits through the fringe field. Material, magnetic environment and radiation resistance are quantitatively linked in [7]. The 'EH' grade of material was selected to further reduce sensitivity by increasing the reverse H_{cj} field required for irreversible magnetisation loss.

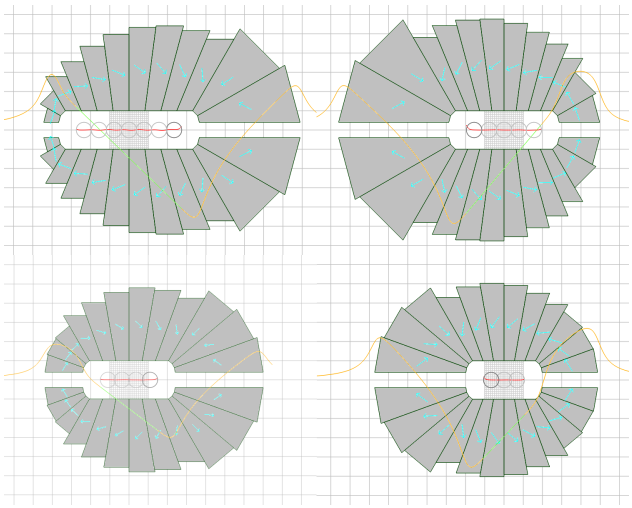

Figure 4: Magnet cross-sections for BF (left) and BD (right) in FFA1 (top) and FFA2 (bottom). Grid has 1 cm spacing and blue arrows denote magnetisation direction.

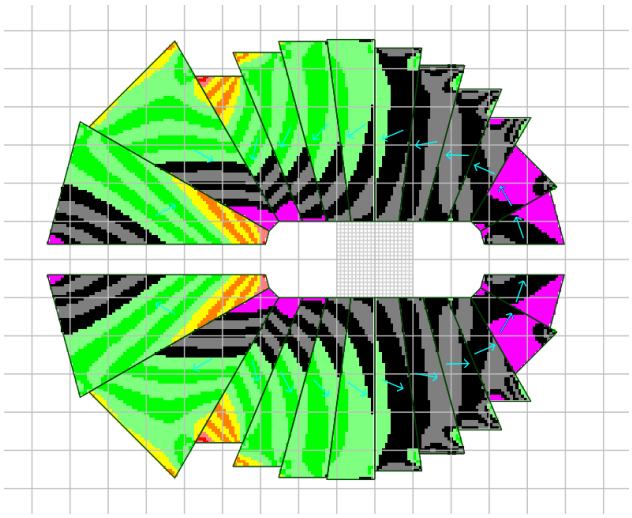

Figure 5: Sensitivity to demagnetisation in the FFA1 BD magnet, given by field antiparallel to the magnetisation direction, $-\mu_0 \mathbf{H}\cdot\mathbf{M}/|\mathbf{M}|$. Black is 0–0.5 T, green ≤1 T, yellow ≤1.5 T and red >1.5 T. Magneta indicates parallel field.

FUTURE WORK

A Laboratory-Directed R&D (LDRD) study is underway at BNL that intends to build short segments of magnets with these parameters, measure their field maps and correct the integrated fields by adapting the method in [5]. Currently, permanent magnet wedges have been ordered but the manufacturing plant in Shanghai is closed due to lockdowns. A Hall probe with ±0.005% accuracy has been purchased and used successfully with a 2D field mapping stage, measuring integrated fields to 1 unit resolution on a test magnet, so this project is in a good position when the magnet pieces arrive.

The design ordered for the LDRD also introduced a 12° incline on the open midplanes to allow a more rigid vacuum chamber that is thicker in most places.

REFERENCES

[1] S. A. Bogacz *et al.*, "20-24 GeV FFA CEBAF Energy Upgrade", presented at the 12th Int. Particle Accelerator Conf. (IPAC'21), Campinas, Brazil, May 2021, paper MOPAB216, pp. 715–718.

[2] R. M. Bodenstein *et al.*, "Current Statuse of the FFA@CEBAF Energy Upgrade Study", presented at the 13th Int. Particle Accelerator Conf. (IPAC'22), Bangkok, Thailand, June 2022, this conference.

[3] G. H. Hoffstaetter *et al.*, "CBETA Design Report, Cornell-BNL ERL Test Accelerator", 2017. arXiv:1706.04245

[4] A. Bartnik *et al.*, "CBETA: First Multipass Superconducting Linear Accelerator with Energy Recovery", *Phys. Rev. Lett.*, vol. 125, p. 044803, 2020. doi:10.1103/PhysRevLett.125.044803

[5] S. Brooks, G. Mahler, J. Cintorino, J. Tuozzolo, and R. Michnoff, "Permanent magnets for the return loop of the Cornell-Brookhaven energy recovery linac test accelerator", *Phys. Rev. Accel. Beams*, vol. 23, p. 112401, Nov 2020. doi:10.1103/PhysRevAccelBeams.23.112401

[6] S. J. Brooks, "Modified Halbach Magnets for Emerging Accelerator Applications", presented at the 12th Int. Particle Accelerator Conf. (IPAC'21), Campinas, Brazil, May 2021, paper TUXC07, pp. 1315–1318.

[7] A.B. Temnykh, "Measurement of NdFeB permanent magnets demagnetization induced by high energy electron radiation", NIM A **587**, pp. 13–19, 2008.